

Mixed calcium-magnesium pre-nucleation clusters enrich calcium

Andreas Verch^{II}, Markus Antonietti^{II} and Helmut Cölfen^{*,I}

^I Physical Chemistry, POB 714, Universität Konstanz, Universitätsstr. 10, D-78457 Konstanz, Germany

^{II} Colloid Chemistry, Max Planck Institute of Colloids and Interfaces, Am Mühlenberg 1, D-14476 Potsdam-Golm, Germany

Received February 20, 2012; accepted August 31, 2012

Published online: October 15, 2012

Pre-nucleation cluster / Amorphous calcium carbonate / Preferential ion binding / Mg-calcite / Non classical nucleation

Abstract. It is demonstrated that magnesium and carbonate ions can form pre-nucleation clusters in analogy to calcium carbonate. If a mixed calcium and magnesium solution is brought in contact with carbonate ions, mixed pre-nucleation clusters form. The equilibrium constants for their formation are reported revealing that over the entire range of possible cation mixing ratios, calcium gets enriched over magnesium in the pre-nucleation clusters. This can explain high magnesium contents in amorphous calcium carbonate. However, this enrichment alone is not sufficient to explain the magnesium content of less than 41 mol% which is found in magnesium calcite biominerals nucleated from seawater.

1. Introduction

Many marine invertebrates possess a shell or scaffold made of calcium carbonate. Most of these materials comprise the polymorphs aragonite and calcite. Laboratory experiments underline the importance of the $\text{Mg}^{2+}/\text{Ca}^{2+}$ -ratio in the solution regarding both the morphology [1] and the polymorphism [2–4] of the precipitated material. High $\text{Mg}^{2+}/\text{Ca}^{2+}$ -proportions ($>4:1$) for example lead to the formation of aragonite instead of calcite [2–4]. Aragonite usually does not include Mg^{2+} , biogenic Mg-calcite crystals can incorporate up to 41 mol% Mg^{2+} [5]. This integration of Mg^{2+} into calcite is of huge importance regarding the properties and the use of these minerals [6]. Artificial Mg-calcites, however, commonly contain merely 1–3 mol% Mg^{2+} [7]. Mg^{2+} contents observed in synthetic amorphous CaCO_3 (ACC) in contrast can be significantly higher. Wang *et al.* observed that carboxylated molecules might regulate and increase the Mg-content in amorphous CaCO_3 (ACC) [8].

It is meanwhile well accepted that many carbonate biominerals form via amorphous precursor phases [9] including those formed by marine organisms like sea urchins

[10]. Although seawater contains about 5 times more Mg^{2+} than Ca^{2+} [11], Mg-calcites found in biominerals always contain less Mg as compared to Ca [5]. For example, a recent detailed analysis of an adult sea urchin spine revealed only 4 mol-% Mg^{2+} [12]. Although it is clear that the calcite lattice can only accommodate a limited amount of Mg^{2+} ions, the reason for the enrichment of Ca^{2+} over Mg^{2+} can not only be due to lattice constraints. Otherwise, Mg-calcite in marine biominerals would always contain the maximum possible Mg^{2+} amount, especially if it is considered that an amorphous precursor phase can accommodate a much higher Mg^{2+} amount. However, the maximum possible Mg^{2+} amount is obviously not the rule in marine magnesium calcite biominerals.

The reason for the possible Ca^{2+} over Mg^{2+} enrichment can already lie in the earliest formed species in a carbonate precipitation reaction. Although it had been known and extensively studied for already more than 80 years that the activities of Mg^{2+} and Ca^{2+} ions are significantly reduced in the presence of carbonate ions [13, 14] only recent analytical ultracentrifugation (AUC) [14] and cryo-TEM [15] experiments on Ca^{2+} and carbonate ion containing solutions have demonstrated that nm-sized pre-nucleation clusters are present even before the onset of nucleation [16]. These clusters then aggregate [14, 15] in order to subsequently form ACC. It is therefore of interest to reveal the composition of MgCO_3 and CaCO_3 pre-nucleation species in a mixed $\text{Mg}^{2+}/\text{Ca}^{2+}$ carbonate precipitation system to address the question whether a Ca^{2+} enrichment is already found in these pre-nucleation species.

In this paper we present the result of AUC experiments on a pure MgCO_3 solution as well as results from titration experiments on Ca/MgCO_3 systems with varying Mg/Ca-ratios. In these experiments Mg^{2+} and Ca^{2+} containing solutions were added to 10 mM Na_2CO_3 solutions at a constant rate. The Mg^{2+} and Ca^{2+} potentials in solution were recorded by means of ion selective electrodes (ISE). The pH-value was kept constant by adding NaOH solution. Four different Mg/Ca-proportions were investigated ranging from 5:1, which corresponds to the Mg/Ca proportion of seawater [11], over 1:1 and 1:2 down to 1:5. Additionally, we conducted experiments in the pure MgCO_3 and CaCO_3 system, respectively.

* Correspondence author (e-mail: helmut.coelfen@uni-konstanz.de)

Results and discussion

The development of the free Ca^{2+} concentration calculated from the recorded ion potentials is shown in Fig. 1a) for different Mg/Ca-ratios. A comparison of the nucleation times of the reference experiment in the absence of Mg^{2+} and those experiments in the presence of Mg^{2+} reveals that Mg^{2+} delays the nucleation of CaCO_3 like typical low and high molecular nucleation inhibitors [17, 18]. In general, it seems that the retardation of the nucleation is increasing with rising Mg^{2+} proportions. Interestingly, however, the strongest retardation of the nucleation is reproducibly observed in the experiments with the smallest applied Mg/Ca-ratios (1:5 and 1:2). This observation leads to the assumption that apparently two different nucleation pathways must be accessible at lower and higher Mg^{2+} contents. This phenomenon is denoted as bifurcation. A similar behaviour was recently also described for the precipitation of CaCO_3 in the presence of sodium triphosphate [18]. Another important effect in the pre-nucleation stage is the increasing slope of the Ca^{2+} concentration with time prior to nucleation with rising Mg^{2+} proportions. This implies that less calcium is consumed to form CaCO_3 pre-nucleation species at high Mg/Ca-ratios rather than at low Mg concentrations. As the number of carbonate ions is by orders higher than the added amount of Ca^{2+} and Mg^{2+} ions, it can be excluded that solely the increased consumption of carbonate ions is the cause for

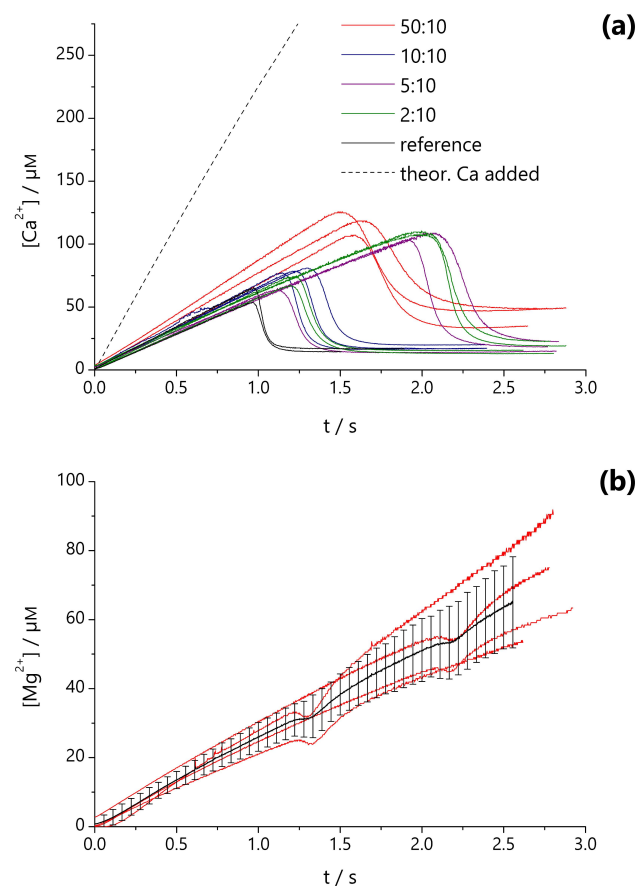


Fig. 1. (a) Development of the detected free calcium concentration and (b) progression of the measured Mg^{2+} concentration at a $\text{Mg}^{2+}/\text{Ca}^{2+}$ ratio in the dosed solution of 2:10 (red, 4 measurements).

this observation. Instead, this effect on the CaCO_3 pre-nucleation equilibrium must be related to the presence of Mg^{2+} . A quantitative analysis of the pre-nucleation equilibria is discussed in more detail further below.

Due to the wide range of Mg^{2+} -concentrations applied in the different experiments, the progression of the free Mg^{2+} concentration is illustrated exemplarily for the experiment with an Mg/Ca-ratio of 2:10. Generally, it is important to note that the data from the magnesium ion selective electrode are less reproducible than those from the Ca-ISE, e.g. the slopes before the nucleation fluctuate significantly stronger between the single measurements (Fig. 1b). Hence, we used averaged values of different measurements to increase the statistical significance (not shown). At this low Mg^{2+} concentration the CaCO_3 nucleation can be identified by a sudden but short decline and a subsequent steeper rise in the free Mg^{2+} concentration. The initial drop of the Mg^{2+} concentration is presumably an artifact of the low selectivity of the Mg ion selective electrode towards Ca^{2+} . At the highest Mg/Ca-ratios this drop is not detected. However, in general the free amount of Mg^{2+} ions rises significantly faster after nucleation, while the Ca^{2+} concentration drops to the level, which corresponds to an equilibrium of amorphous CaCO_3 . This indicates a resolubilization of Mg^{2+} ions from pre-nucleation clusters upon nucleation. Two explanations for this observation are feasible: 1) The concentration of carbonate ions decreases rapidly after the nucleation, which triggers an adoption of the MgCO_3 pre-nucleation equilibrium. Due to the large excess of carbonate ions, this possibility is unlikely. 2) Mg^{2+} ions, which were incorporated into then precipitated pre-nucleation species, are released during the mineralization process leading to an increased number of free Mg^{2+} ions (see below). After nucleation, the slope in the time dependence of free $[\text{Mg}^{2+}]$ lowers a bit but is still steeper than before the nucleation, which likewise might be caused by both aforementioned reasons.

In all conducted experiments the Mg^{2+} ions influenced the polymorph, which was mineralized. Even at the lowest Mg/Ca-ratios solely aragonite was found. In contrast, in experiments in the absence of Mg^{2+} ions both calcite and vaterite were isolated 1 hr after the nucleation. An influence of the two supposed nucleation modes at lower $\text{Mg}^{2+}/\text{Ca}^{2+}$ -proportions on the precipitated mineral polymorph could not be identified; in both cases aragonite is formed. However, the reproducible differences in the nucleation times indicate that the mineralization proceeds via different intermediate species [18], though they cannot be identified by the technique we applied in this study. Indication for the formation of Mg-calcite could not be found.

A quantitative analysis of the formation of MgCO_3 and CaCO_3 pre-nucleation species at different Mg/Ca-ratios is shown in Fig. 2. The formation constants K_{Ca} and K_{Mg} were calculated assuming the binding of one carbonate with one Mg^{2+} and Ca^{2+} ion, respectively. Here, the free cation concentrations were known from the recorded Mg^{2+} resp. Ca^{2+} ion potentials at the given $\text{pH} = 9.75$. $[\text{CaCO}_3]$ resp. $[\text{MgCO}_3]$ was accessible via the difference between added and detected cations prior to nucleation assuming a 1:1 stoichiometry between bound cations and

anions. The free carbonate ion concentration could be determined via subtracting $[\text{CaCO}_3]$ and $[\text{MgCO}_3]$ from the known initial carbonate concentration.

$$K_{\text{Ca}} = \frac{[\text{CaCO}_3]}{[\text{Ca}^{2+}][\text{CO}_3^{2-}]} ; \quad K_{\text{Mg}} = \frac{[\text{MgCO}_3]}{[\text{Mg}^{2+}][\text{CO}_3^{2-}]}$$

The above equilibrium constants refer to ion pairs but as it is known that CaCO_3 pre-nucleation clusters are composed of an equal number of cations and anions [14], it is reasonable to assume similar conditions for MgCO_3 pre-nucleation clusters. The determined constants for the formation of CaCO_3 and MgCO_3 pre-nucleation species in pure systems are in good agreement with previous studies [19–21]. In an ideal system without the formation of mixed pre-nucleation clusters, one would expect that Mg^{2+} and Ca^{2+} containing species act independently from each other, so that the equilibrium constants do not change with altering Mg/Ca-ratios. The development of the formation constant of CaCO_3 pre-nucleation species with rising Mg-contents illustrates however that the presence of Mg^{2+} indeed influences the stability of CaCO_3 pre-nucleation species (Fig. 2).

The higher the Mg/Ca-proportion the smaller is the formation constant K_{Ca} . The same trend can be observed for MgCO_3 pre-nucleation species. This observation is unexpected when assuming that solely ion pairs or pure MgCO_3 and CaCO_3 pre-nucleation species are formed as the formation constants K_{Ca} and K_{Mg} had to be constant independently from the Mg/Ca-ratio in the solution. Though, a feasible explanation of this behaviour is that Mg^{2+} interacts with CaCO_3 pre-nucleation species and vice versa.

Hence, exclusively pure CaCO_3 and MgCO_3 pre-nucleation species are obviously not formed in favour of mixed pre-nucleation cluster formation. This finding is understandable since Mg^{2+} and Ca^{2+} ions are chemically similar and can replace each other as the well-known example of Mg-calcite shows. After formation of mixed pre-nucleation clusters, the stability of the respective Ca-pre-nucleation species is apparently reduced. However, the question if there are two types of clusters, one high in Ca^{2+} and the other one enriched in Mg^{2+} , cannot be solved on basis of the present data set. Nevertheless, a

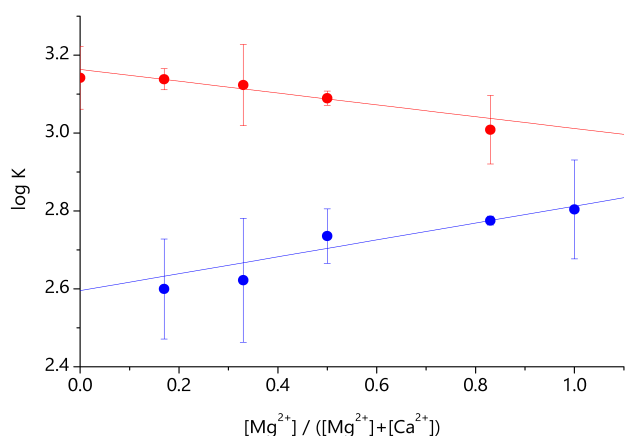


Fig. 2. Development of the equilibrium constants of Mg clusters (blue, squares) and Ca clusters (red, circles), respectively with changing magnesium mole fraction in the dosed solution.

recent theoretical work has shown that CaCO_3 pre-nucleation clusters are highly dynamic forming and dissociating polymeric species [22]. In turn, this means that two different pre-nucleation cluster species, one high in $[\text{Ca}^{2+}]$ and one high in $[\text{Mg}^{2+}]$ should not exist but on time average only a single mixed species with uniform composition.

Mixed pre-nucleation species, containing both Mg^{2+} and Ca^{2+} might also explain how ACC with high Mg^{2+} -ratios can be formed since pre-nucleation clusters are the constituents of the then precipitated amorphous phase as indicated for CaCO_3 [14, 15].

In order to elucidate the existence of MgCO_3 pre-nucleation clusters as well as mixed clusters, AUC-experiments were conducted in solely Mg^{2+} containing carbonate solutions as well as carbonate solutions containing both Mg^{2+} and Ca^{2+} ions (ratio 5:1). The recorded data were analyzed applying the model of discrete non-interacting species via fitting of the experimental data to the Lamm equation using the SEDFIT software [23]. In this model the mean value of the sedimentation coefficient s is determined for up to 4 individual species in the solution as well as their diffusion coefficients and concentrations. The sedimentation coefficient is a measure for the sedimentation velocity of particles, which is linked among others to the molar mass, the density and the shape of the subject of investigation. Higher molar mass and/or density lead to a higher s -value. The results of the data analysis are shown in Fig. 3.

In the MgCO_3 -experiments 3 to 4 different species could be detected. The species (S_1) with the lowest sedimentation coefficient ($s_1 < 0.2$ S) represent hydrated ions (magnesium, carbonate, sodium and chloride ions). Generally the resolution is too small to distinguish between different ion species and ion pairs. The next faster sedimenting species (S_2) exhibits a sedimentation coefficient of about 1.0 S. This species is too large to correlate it to a single hydrated ion species. In previous experiments on CaCO_3 , this species was assigned to the pre-nucleation clusters [14]. In addition, up to two even larger species could be detected in the present experiments. These spe-

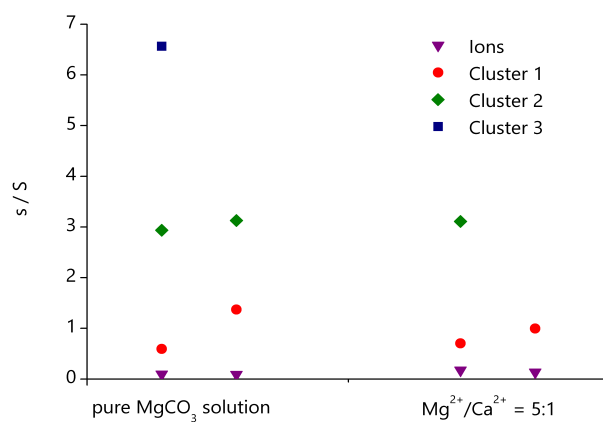


Fig. 3. Sedimentation coefficients s obtained in analytical ultracentrifugation experiments on Mg^{2+} as well as Mg^{2+} and Ca^{2+} containing carbonate buffer solutions. The smallest s -value represents ions and ion pairs, which cannot be separated by means of AUC, while larger sedimentation coefficients represent different cluster species. The experiments were repeated twice for each sample and are displayed in columns.

cies with a sedimentation coefficient s_3 and s_4 are formed by aggregation of the smaller pre-nucleation species as suggested in a previous work [14, 15]. In general, the present results resemble those on the CaCO_3 system [14]. Consequently, in carbonate solutions containing both Mg^{2+} and Ca^{2+} ions cluster species were found, too. The sedimentation coefficient of the species s_2 here again was around $s = 1.0$ S. Hence, no significant differences to the experiments with pure MgCO_3 -solution could be detected. Due to the resolution limit of the AUC it is not possible to make any further statements about the mixed Mg/Ca-pre-nucleation species.

Conclusions

In this study we revealed that in solutions of magnesium and carbonate ions pre-nucleation clusters are formed, as previously already had been shown for the CaCO_3 -system. In pure MgCO_3 solutions different cluster species could be identified besides the expected ions. Experiments in solutions containing both magnesium and calcium ions showed that the stability of CaCO_3 pre-nucleation species tends to decrease, when the Mg^{2+} ion concentration increases. The same trend was found for MgCO_3 clusters in the presence of Ca^{2+} ions. This behavior cannot be explained when pure magnesium or calcium carbonate clusters are assumed. Hence, magnesium and calcium form mixed carbonate clusters. However, the formation constant of CaCO_3 pre-nucleation species stays under all conditions by a factor of > 1 larger than that of MgCO_3 . This means in turn, that mixed clusters are enriched in Ca^{2+} as compared to the solution composition over the entire range of possible cation mixing ratios with the exception of pure Mg^{2+} . Thus, pre-nucleation clusters lead to a Ca^{2+} enrichment with an equilibrium constant, which is larger by a factor 1.5–4 over that of MgCO_3 pre-nucleation clusters (see also Fig. 2) in the pre-nucleation clusters depending on the initial cation mixing ratio. A factor between these equilibrium constants of 1.78 for the 5:1 Mg/Ca mixing ratio in seawater is found. Since the clusters are mixed with respect to both cations and carbonate is present in a large excess and thus constant for both equilibria, the enrichment of Ca^{2+} over Mg^{2+} in the clusters can be calculated by multiplying the equilibrium constants with the concentration of the respective free cations. For the 5:1 mixing ratio, this results in 26 mol% Ca^{2+} bound in the pre-nucleation clusters compared to the 17 mol%, resulting from the initial mixing ratio. However, this still gives a Mg^{2+} amount of 77 mol% in the mixed pre-nucleation clusters for model seawater conditions. This is still much higher than the 41 mol% maximum Mg-content in biogenic Mg-calcite [5]. Therefore, Ca^{2+} enrichment in pre-nucleation clusters is not the only factor to explain the enrichment of Ca^{2+} in biogenic magnesium calcite precipitated from seawater alone. Potential deviations may result from the fact that the pH of seawater is lower than the here applied $\text{pH} = 9.75$ or the situation that there are a number of further ions in real seawater, which may also get incorporated into mixed pre-nucleation clusters thus changing their stability.

The formation of calcium and magnesium mixed pre-nucleation clusters nevertheless illustrates how huge amounts of Mg^{2+} can be incorporated into amorphous CaCO_3 with these pre-nucleation clusters being the nucleation relevant species and precursor of ACC [14, 15]. In the following crystallisation steps, hydration energies, lattice constraints or potentially present crystallisation modifiers may play a further key role in determining the polymorphism and the Mg-content of the final crystal.

Experimental section

All experiments were performed at 24 ± 1 °C. The preparation of the solutions, the titration setup and the experimental procedure including the appropriate calibration procedures are described somewhere else in detail [14, 17]. The following chemicals were purchased and used without further purification: 1 N HCl (No: 1.09057.1000; Merck) and NaOH (No: 1.09137.1000; Merck), NaHCO_3 (99.7%; No. 424270010; Acros Organics), Na_2CO_3 (anhydrous, 99.95%; No. 223484; Sigma-Aldrich), $\text{CaCl}_2 \cdot 2 \text{H}_2\text{O}$ (99.5%; No. 21097; Fluka) and $\text{MgCl}_2 \cdot 6 \text{H}_2\text{O}$ (>99%, Roth, Nr. 2189.2). All experiments were performed in a beaker (50 mL) equipped with a stirring bar and filled with a carbonate buffer solution (10 mm) at $\text{pH} 9.75$. Solutions containing CaCl_2 (10 mm) and MgCl_2 in different ratios were preset to $\text{pH} = 9.75$ by addition of 10 mm NaOH-solution (the dilution due to the pH-adjustment is considered), and subsequently added to the buffer solution at a constant rate of 0.01 mL/min while the Ca^{2+} and Mg^{2+} -potentials were recorded by means of electrodes selective to the respective ions. The pH-value is kept constant during the experiment via pH-constant titration. After every experiment, beaker, burette tips and electrodes were washed with acetic acid (10%) and carefully rinsed with distilled water. Analytical ultracentrifugation experiments were performed on a Beckman-Coulter XL-I Ultracentrifuge using Rayleigh interference optics at 25 °C and 60,000 RPM. An experiment lasted at least 8 hr. AUC data were analysed using SEDFIT [23] software applying the model of discrete non-interacting species.

Acknowledgements. We thank Antje Völkel, who conducted the AUC experiments and the data evaluation, as well as the Max-Planck Society for the financial support.

References

- [1] E. Loste, R. M. Wilson, R. Seshadri, F. C. Meldrum, *J. Cryst. Growth* **2003**, 254, 206–218.
- [2] Y. Kitano, *Bull. Chem. Soc. Jpn.* **1962**, 35, 1973–1980.
- [3] S. Raz, S. Weiner, L. Addadi, *Adv. Mater.* **2000**, 12, 38–42.
- [4] A. Mucci, J. W. Morse, *Geochimica Et Cosmochimica Acta* **1983**, 47, 217–233.
- [5] J. H. Schroeder, E. J. Dwornik, J. J. Papike, *Geol. Soc. Am. Bull.* **1969**, 80, 1613–1616.
- [6] Y. R. Ma, B. Aichmayer, O. Paris, P. Fratzl, A. Meibom, R. A. Metzler, Y. Politi, L. Addadi, P. Gilbert, S. Weiner, *Proc. Natl. Acad. Sci. USA* **2009**, 106, 6048–6053.

- [7] Y. Politi, D. R. Batchelor, P. Zaslansky, B. F. Chmelka, J. C. Weaver, I. Sagi, S. Weiner, L. Addadi, *Chemistry of Materials* **2010**, *22*, 161–166.
- [8] D. B. Wang, A. F. Wallace, J. J. De Yoreo, P. M. Dove, *Proc. Natl. Acad. Sci. USA* **2009**, *106*, 21511–21516.
- [9] S. Weiner, I. Sagi, L. Addadi, *Science* **2005**, *309*, 1027–1028.
- [10] Y. Politi, T. Arad, E. Klein, S. Weiner, L. Addadi, *Science* **2004**, *306*, 1161–1164.
- [11] DOE, *Handbook of methods for the analysis of the various parameters of the carbon dioxide system in sea water*, 2. ed., ORNL/CDIAC-74 **1994**.
- [12] J. Seto, Y. Ma, S. A. Davis, F. Meldrum, A. Gourrier, Y. Y. Kim, U. Schilde, M. Sztucki, M. Burghammer, S. Maltsev, C. Jäger, H. Cölfen, *Proc. Natl. Acad. Sci. USA* **2012**, *109*, 3699–3704.
- [13] R. Money, C. W. Davies, *Trans. Faraday Soc.* **1932**, *28*, 609–614.
- [14] D. Gebauer, A. Völkel, H. Cölfen, *Science* **2008**, *322*, 1819–1822.
- [15] E. M. Pouget, P. H. H. Bomans, J. Goos, P. M. Frederik, G. de With, N. Sommerdijk, *Science* **2009**, *323*, 1455–1458.
- [16] D. Gebauer, H. Cölfen, *Nano Today* **2012**, *6*, 564–584.
- [17] D. Gebauer, H. Cölfen, A. Verch, M. Antonietti, *Adv. Mater.* **2009**, *21*, 435–439.
- [18] A. Verch, D. Gebauer, M. Antonietti, H. Cölfen, *Physical Chemistry Chemical Physics* **2011**, *13*, 16811–16820.
- [19] R. M. Siebert, P. B. Hostetler, *Am. J. Sci.* **1977**, *277*, 716–734.
- [20] E. J. Reardon, D. Langmuir, *Am. J. Sci.* **1974**, *274*, 599–612.
- [21] L. N. Plummer, E. Busenberg, *Geochimica Et Cosmochimica Acta* **1982**, *46*, 1011–1040.
- [22] R. Demichelis, P. Raiteri, J. D. Gale, D. Quigley, D. Gebauer, *Nature Communications* **2012**, *2*.
- [23] P. Schuck, *Biophysical Journal* **2000**, *78*, 1606–1619.